

“Bi-modal” Isoscalar Giant Dipole Strength in ^{58}Ni

B.K. Nayak, U. Garg, M. Hedden, M. Koss, T. Li, Y. Liu, P.V. Madhusudhana Rao, S. Zhu
Physics Department, University of Notre Dame, Notre Dame, IN 46556, USA

M. Itoh, H. Sakaguchi, H. Takeda, M. Uchida, Y. Yasuda, M. Yosoi
Department of Physics, Kyoto University, Kyoto 606-8502, Japan

H. Fujimura, M. Fujiwara, K. Hara
*Research Center for Nuclear Physics, Osaka University,
Mihogaoka 10-1 Ibaraki, Osaka 567-0047, Japan*

T. Kawabata
*Center for Nuclear Study, Graduate School of Science,
University of Tokyo, Bunkyo, Tokyo 113-0033, Japan*

H. Akimune
Department of Physics, Konan University, Kobe, Hyogo 658-8501, Japan

M.N. Harakeh
*Kernfysisch Versneller Instituut, University of Groningen,
9747 AA Groningen, The Netherlands*

(Dated: August 17, 2018)

Abstract

The strength distribution of the isoscalar giant dipole resonance (ISGDR) in ^{58}Ni has been obtained over the energy range 10.5–49.5 MeV via extreme forward angle scattering (including 0°) of 386 MeV α particles. We observe a “bi-modal” $E1$ strength distribution for the first time in an $A < 90$ nucleus. The observed ISGDR strength distribution is in good agreement with the predictions of a recent RPA calculation.

PACS numbers: 24.30.Cz, 21.65.+f, 25.55.Ci, 27.40+z

The compressional-mode giant resonances in the atomic nuclei—the isoscalar giant monopole resonance (ISGMR) and the isoscalar giant dipole resonance (ISGDR)—provide a direct method to obtain the incompressibility of the nucleus and of nuclear matter (K_{nm}) [1]. Although ISGMR has been investigated extensively for a large number of nuclei in the past, the exotic ISGDR has been identified only in a few nuclei and the location of ISGDR is not systematically established over the wide mass region. One major concern with ISGDR data had been that the nuclear incompressibility extracted from the centroid of the ISGDR strength distribution was significantly different from that obtained from the ISGMR data. In recent work, this ambiguity has been resolved for ^{208}Pb by a more precise, background-free measurement of ISGDR strength distribution, and the value of K_{nm} obtained from the ISGMR data is now consistent with that from the ISGDR data for ^{208}Pb [2].

The experimentally-observed ISGDR strength distribution in all $A \geq 90$ nuclei has a “bi-modal” structure [3, 4, 5, 6], in agreement with predictions of recent theoretical work [7, 8, 9, 10]. Of these, only the high-energy (HE) component depends on K_{nm} and, hence, is of interest from the point of view of determining an experimental value for this important parameter. The low-energy (LE) component, which is quite small in comparison with the HE component, is located much higher in excitation energy than the expected $1\hbar\omega$ component of the ISGDR, previously identified by Poelhekkens *et al.*[11]. As well, it is lower in energy than the isovector giant dipole resonance (IVGDR) which can be excited in inelastic α scattering via Coulomb excitation; in the event, the full expected IVGDR strength is subtracted out in the analysis of all aforementioned data. The exact nature of this component is not fully understood yet, although suggestions have been made that it might represent the “toroidal” or “vortex” modes; Refs. [12, 13] provide a review of the recent experimental and theoretical results on ISGDR.

For ^{58}Ni , there has been only one recent measurement, wherein a concentrated ISGMR and isoscalar giant quadrupole resonance (ISGQR) strength distribution has been observed, but the ISGDR strength is reported to be spread more or less uniformly over $E_x = 12$ to 35 MeV [14]. This observation leaves a few open questions: Is the ISGDR strength fragmented in light nuclei such as ^{58}Ni ? Are we missing the resonance strength distribution because of experimental limitations? In an attempt to answer these questions, we have carried out measurements on excitation of isoscalar giant resonances in ^{58}Ni . In this Letter, we report our results on the ISGDR strength distribution in ^{58}Ni . We find that the ISGDR in this

nucleus has a “bi-modal” structure as well, similar to that in the medium- and heavy-mass nuclei, and that the experimentally observed ISGDR strength is in good agreement with predictions of a recent RPA calculation.

The $^{58}\text{Ni}(\alpha, \alpha')$ experiment at $E_\alpha = 386$ MeV was performed at the ring-cyclotron facility of Research Center for Nuclear Physics (RCNP), Osaka University. Details of the experimental measurements and data analysis procedures have been provided in Refs. [2, 4]; only the salient points are elaborated upon below. α -particles, inelastically scattered off a 5.8 mg/cm²-thick ^{58}Ni target, were momentum analyzed in the spectrometer, Grand Raiden [15], and detected in the focal-plane detector system comprised of two multi-wire drift-chambers and two scintillators, providing particle identification as well as the trajectories of the scattered particles. The scattering angle at the target and the momentum of a scattered particle were determined by the ray-tracing method. The $^{58}\text{Ni}(\alpha, \alpha')$ spectra were measured in the angular range of 0° to 8.5° for two excitation-energy-bite settings of the spectrometer ($E_x = 5.0$ – 35.0 MeV and $E_x = 22.0$ – 52.0 MeV). The primary beam was stopped at one of four different Faraday cups, depending on the scattering angle and the excitation energy bite of the spectrometer. The vertical position spectrum obtained in the double-focused mode of the spectrometer was exploited to eliminate the instrumental background due to Coulomb scattering of the beam at the target and subsequent rescattering by the edges of the entrance slit, the yoke, and walls of the spectrometer [2, 4]. Fig. 1 shows an excitation energy spectrum for the $^{58}\text{Ni}(\alpha, \alpha')$ reaction at $\theta_{avg.} = 0.69^\circ$ after subtraction of the instrumental background. A prominent “bump” corresponding to (ISGMR + ISGQR) in ^{58}Ni is observed at $E_x = 10$ – 25 MeV and another bump [ISGDR + the high-energy octupole resonance (HEOR)] is visible as a shoulder at $E_x \sim 33$ MeV. There is an underlying continuum in the high excitation-energy region in the spectrum. Since there is no sound theoretical basis to estimate and subtract the physical continuum from the excitation energy spectrum, it is reasonable to assume that the continuum background remaining after elimination of the instrumental background is the contribution from the higher multipoles and the three-body channels resulting, for example, from knock-out reaction. In the present work, a multipole-decomposition (MD) analysis has been performed to extract giant resonance strengths, by taking into account the transferred angular momentum up to $\Delta L = 7$. The cross-section data were binned in 1-MeV energy intervals to reduce the statistical fluctuations. For each excitation-energy bin from 10.5 MeV to 49.5 MeV, the experimental

angular distribution $\sigma^{exp}(\theta_{c.m.}, E_x)$ has been fitted by means of the least-square method with the linear combination of calculated distributions $\sigma^{cal}(\theta_{c.m.}, E_x)$ defined by:

$$\sigma^{exp}(\theta_{c.m.}, E_x) = \sum_{L=0}^{L=7} a_L(E_x) \times \sigma_L^{cal}(\theta_{c.m.}, E_x), \quad (1)$$

where $\sigma_L^{cal}(\theta_{c.m.}, E_x)$ is the calculated distorted-wave Born approximation (DWBA) cross section corresponding to 100% energy-weighted sum rule (EWSR) for the L^{th} multipole.

The DWBA calculations were performed following the method of Satchler and Khoa [16] using density-dependent single folding, with a Gaussian α -nucleon potential (range $t = 1.88$ fm) for the real part, and a Woods-Saxon imaginary term; the calculations were carried out with the computer code PTOLEMY [17]. Input parameters for PTOLEMY were modified [18] to take into account the correct relativistic kinematics. The shape of the real part of the potential and the form factors for PTOLEMY were obtained using the codes SDOLFIN and DOLFIN [19]. We used the transition densities and sum rules for various multipolarities described in Refs. [1, 20]. The radial moments for ^{58}Ni were obtained by numerical integration of the Fermi mass distribution with $c = 4.08$ fm and $a = 0.515$ fm [20]. The folding-model parameters with the computer code PTOLEMY were obtained from analysis of $^{58}\text{Ni} + \alpha$ elastic- and $J^\pi = 2^+$ inelastic-scattering data at $E_\alpha = 386$ MeV taken in a separate experiment. The folding model parameter extracted for the real part of the potential is $V = 37.02$ MeV, and the parameters for the Woods-Saxon type imaginary part were: $W = 36.86$ MeV, r_I (reduced radius) = 0.95 fm, and a_I (diffuseness) = 0.67 fm. Using these parameters, the DWBA calculation for the first $J^\pi = 2^+$ state in ^{58}Ni was carried out with PTOLEMY using a collective form factor with the previously-known $B(E2) = 0.070$ e²b² [21, 22]. Fig. 2 compares the results of the calculations and the experimental data; the calculations reproduce elastic scattering cross sections as well as the inelastic scattering differential cross section for the 2^+ state very well.

The contribution of the IVGDR excitation to the measured cross sections was subtracted prior to multipole decomposition. The cross section for IVGDR excitation was calculated using the strength distribution obtained from photonuclear work [23] in conjunction with DWBA calculations on the basis of the Goldhaber-Teller model. The fits of the angular distributions for two energy bins near the peaks of the ISGMR and ISGDR are shown in Fig. 3; the $L = 0, 1, 2$ and 3 contributions to the differential cross section are also shown.

The ISGMR has a maximum at $\theta_{c.m.} = 0^\circ$ and its contribution is dominant in comparison to the other multipoles at $E_x = 18.5$ MeV. Similarly, the ISGDR has a maximum at $\theta_{c.m.} \sim 2^\circ$ and its contribution is dominant in comparison to the other multipoles at 29.5 MeV. The fitted parameters $a_L(E_x)$ so obtained are fractions of the EWSR's, which can be related to the strengths $S_L(E_x)$ as follows:

$$S_0(E_x) = \frac{2\hbar^2 A \langle r^2 \rangle}{mE_x} a_0(E_x), \quad (2)$$

$$S_1(E_x) = \frac{3\hbar^2 A}{8\pi m E_x} \left(11 \langle r^4 \rangle - \frac{25}{3} \langle r^2 \rangle^2 - 10\epsilon \langle r^2 \rangle \right) a_1(E_x), \quad (3)$$

$$S_{\geq 2}(E_x) = \frac{\hbar^2 A}{8\pi m E_x} L(2L+1)^2 \langle r^{2L-2} \rangle a_L(E_x), \quad (4)$$

where m , A , and $\langle r^N \rangle$ are the nucleon mass, the mass number, the N^{th} moment of the ground-state density, respectively, and $\epsilon = (4/E_2 + 5/E_0)\hbar^2/3mA$. E_0 and E_2 are the centroid energies of the GMR and GQR, respectively. The strength distributions extracted from these fits for $L = 0$ (ISGMR), $L = 1$ (ISGDR), and $L = 2$ (ISGQR) in ^{58}Ni are shown in Fig. 4. In order to examine the reliability of the strength distributions obtained from the fits in the MD analysis, we varied the L_{max} value from $L = 6$ to $L = 8$. However, the extracted strength distributions for $L = 0-3$ did not change in any significant way. In addition, a completely independent data analysis, using a different folding-model potential, led to essentially the same results for the various strength distributions.

The centroid energy of ISGMR, shown in Fig. 4(a), was determined to be $E_x = 19.9_{-0.8}^{+0.7}$ MeV between $E_x = 10.5$ and 32.5 MeV. A total of $92_{-3}^{+4}\%$ of the $E0$ EWSR was identified in the above excitation-energy range. [The errors quoted in all EWSR values here are only statistical; in addition, there may be a 15–20% systematic error in the EWSR fractions because of the uncertainties associated with the DWBA calculations used in the MDA analysis.] This result is similar to that reported earlier [14], where the fraction of $74_{-12}^{+22}\%$ for the $E0$ EWSR value is observed between $E_x = 12.0$ to 31.1 MeV with a centroid of $20.30_{-0.14}^{+1.69}$ MeV.

The strength distribution of ISGDR is shown in Fig. 4(b). We observe a “bi-modal” strength distribution between $E_x = 10.5$ and 42.5 MeV. A low-energy (LE) component at ~ 16 MeV appears as a shoulder at the low-energy side of the extracted ISGDR strength. The

excitation energy of this component is much higher than that expected for the previously-mentioned $1\hbar\omega$ component of the ISGDR [11], and lower than that of the IVGDR ($E_x = 18$ MeV [23]). This is the first observation of concentrated “bi-modal” isoscalar $E1$ resonance in an $A < 90$ nucleus. In the previous measurement on ISGDR strength distribution in ^{58}Ni [14], it was reported that 41% $E1$ EWSR was spread more or less uniformly over $E_x = 12$ to 35 MeV. In the present case, not only is the ISGDR strength concentrated and has a “bi-modal” distribution similar to that observed in the $A \geq 90$ nuclei, it would appear that nearly all of the expected ISGDR strength has been observed: A total of $98^{+4}_{-5}\%$ of the $E1$ EWSR was identified between $E_x = 20.5$ and 40.5 MeV. The centroid energy of the ISGDR for the same excitation energy range is determined to be $30.8^{+1.7}_{-1.1}$ MeV. The difference between the present result and the result of Ref. [14] might be attributable to the fact that in Ref. [14] the multipole decomposition is carried out after subtracting a “background” from the excitation energy spectrum, whereas, as pointed out earlier, no such subtraction is required in the present analysis since our spectra have been rendered free of all instrumental background.

The ISGQR strength distribution is shown in Fig. 4(c). In this case, $73^{+3}_{-3}\%$ of the $E2$ EWSR value has been observed in the excitation energy range between $E_x = 10.5$ –21.5 MeV. The centroid energy of ISGQR is determined to be $16.3^{+0.8}_{-0.9}$. This result is consistent with the result of Ref. [14], where $E2$ strength corresponding to $115 \pm 18\%$ of the $E2$ EWSR was found between $E_x = 10.5$ –20.5 MeV with a centroid of 16.1 ± 0.3 MeV and rms width of 2.4 ± 0.2 MeV. The ISGQR strength shows a near constant value beyond $E_x = 20$ MeV. At present, the reasons behind this extra strength are not fully understood. Similarly, enhanced $E1$ strengths at high excitation energies have been noted previously in other nuclei [3, 4], and have been attributed to contributions to the continuum from three-body channels, such as knock-out reactions. These processes are only implicitly included in the MD analysis as background and may lead to spurious contribution to the extracted giant resonance strengths at higher energies where the associated cross sections are very small. This conjecture is supported by recent charged-particle decay measurements on ISGDR wherein no such spurious strength at high excitation energies is observed [12, 24]. Incidentally, a similar increase at higher excitation energies has also been reported recently in $E0$ strength in ^{12}C [25], when a multipole decomposition was carried out without subtracting the continuum from the excitation-energy spectra.

To get a quantitative understanding of ISGDR strength distribution, the experimental strength distribution has been compared with the predictions of quasi-particle random phase approximation (QRPA) [13] as shown in Fig. 5. The agreement between the experimental and theoretical ISGDR strength distributions is rather good, except at the very highest excitation energies where, as mentioned previously, the experimentally extracted ISGDR strength is compromised by the limitations of the MD analysis procedure. This is quite remarkable since, in general, the details of the theoretical strength distributions do not quite match the experiment even when the centroid energies are in agreement with the experimental data.

In summary, we have performed $^{58}\text{Ni}(\alpha, \alpha')$ measurements at $E_\alpha = 386$ MeV to study the excitation of ISGDR. The ISGDR strength distribution has been obtained up to $E_x = 49.5$ MeV by multipole-decomposition analysis. A two-component ISGDR strength distribution has been observed for the first time in ^{58}Ni and, indeed, in any $A < 90$ nucleus. The centroid energy of the high-energy component of the ISGDR ($E_x = 30.8_{-1.1}^{+1.7}$ MeV) is consistent with the global systematics and the strength distribution for the HE component of the ISGDR is in good agreement, qualitatively and quantitatively, with predictions of QRPA calculations with a nuclear matter incompressibility value of $K_{nm} = 217$ MeV [26].

This work has been supported in part by the US-Japan Cooperative Science Program of JSPS and the US National Science Foundation (grants number INT03-42942 and PHY04-57120).

-
- [1] M.N. Harakeh and A. van der Woude, *Giant Resonances: Fundamental High-Frequency Modes of Nuclear Excitations* (Oxford University Press, New York, 2001), and reference therein.
- [2] M. Uchida *et al.*, Phys. Lett. B **557** (2003) 12.
- [3] M. Uchida *et al.*, Phys. Rev. C **69** (2004) 051301(R).
- [4] M. Itoh *et al.*, Phys. Rev. C **68** (2003) 064602.
- [5] D.H. Youngblood *et al.*, Phys. Rev. C **69** (2004) 034315.
- [6] D.H. Youngblood *et al.*, Phys. Rev. C **69** (2004) 054312.
- [7] G. Colò *et al.*, Phys. Lett. B **485** (2000) 362.
- [8] D. Vretenar, A. Wandelt, and P. Ring, Phys. Lett. B **487** (2000) 334.
- [9] J. Piekarewicz, Phys. Rev. C **64** (2001) 024307.
- [10] S. Shlomo and A.I. Sanzhur, Phys. Rev. C **65** (2002) 044310.
- [11] T.D. Poelheken *et al.*, Phys. Lett. B **278** (1992) 423.
- [12] U. Garg, Nucl. Phys. A **731** (2004) 3.
- [13] G. Colò, Nucl. Phys. A **731** (2004) 15.
- [14] Y.-W. Lui, H.L. Clark, and D.H. Youngblood, Phys. Rev. C **61** (2000) 067307; RIKEN Review **23** (1999) 159.
- [15] M. Fujiwara *et al.*, Nucl. Instrum. Methods Phys. Res. A **422** (1999) 484.
- [16] G.R. Satchler and Dao T. Khoa, Phys. Rev. C **55** (1997) 285.
- [17] M. Rhoades-Brown, M.H. Macfarlane, and S.C. Pieper, Phys. Rev. C **21** (1980) 2417.
- [18] G.R. Satchler, Nucl. Phys. A **540** (1992) 533.
- [19] L.D. Rickerston, The folding program DOLFIN, 1976 (unpublished).
- [20] G.R. Satchler, Nucl. Phys. A **472** (1987) 215.
- [21] S. Raman, C.H. Malarkey, W.T. Milner, C.W. Nestor, and P.H. Stelson, At. Data Nucl. Data Tables **36** (1987) 1.
- [22] R.H. Spear, At. Data Nucl. Data Tables **42** (1989) 55.
- [23] S.S. Dietrich and B.L. Berman, At. Data Nucl. Data Tables **38** (1988) 199.
- [24] M. Hunyadi *et al.*, Phys. Lett. B **576** (2003) 253.
- [25] B. John *et al.*, Phys. Rev. C **68** (2003) 014305.
- [26] G. Colò, N. Van Giai, P.F. Bortignon, and M.R. Quaglia, Phys. Lett. B **485** (2000) 326.

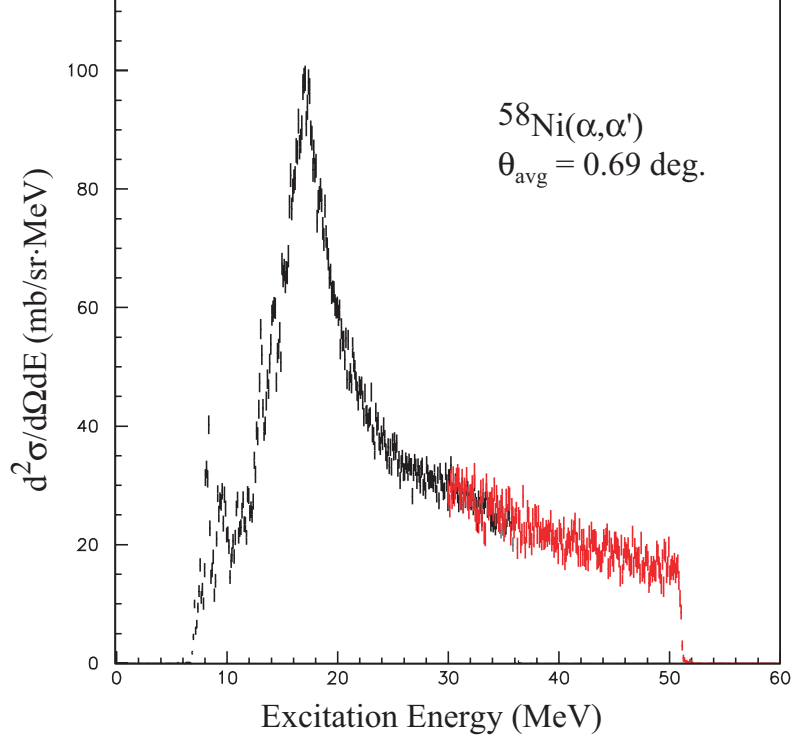


FIG. 1: Excitation energy spectrum for the $^{58}\text{Ni}(\alpha, \alpha')$ reaction at $E_\alpha = 386$ MeV. Inelastically-scattered α particles were measured with the magnetic spectrometer at $\theta = 0^\circ$ with two different settings of the magnetic field to cover the excitation-energy ranges of $E_x = 5.0\text{--}35.0$ MeV and $E_x = 22.0\text{--}52.0$ MeV.

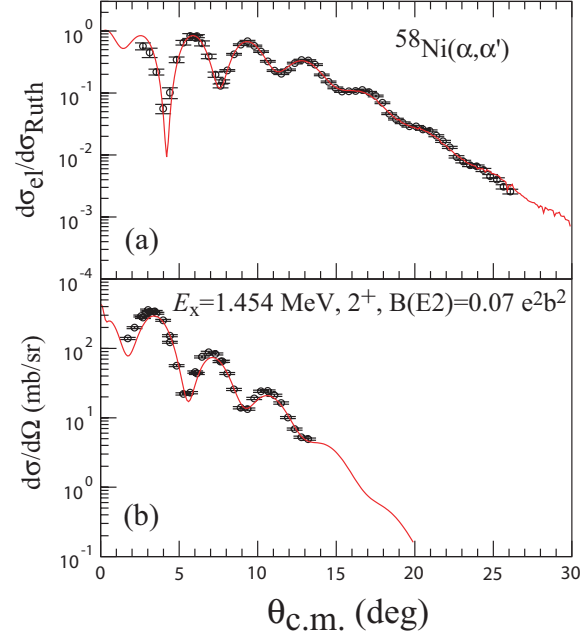


FIG. 2: Cross sections for (a) the $\alpha + ^{58}\text{Ni}$ elastic scattering and (b) the $^{58}\text{Ni}(\alpha, \alpha')^{58}\text{Ni}(2^+)$ reaction at $E_\alpha = 386 \text{ MeV}$. The solid lines are the results of the folding model calculations.

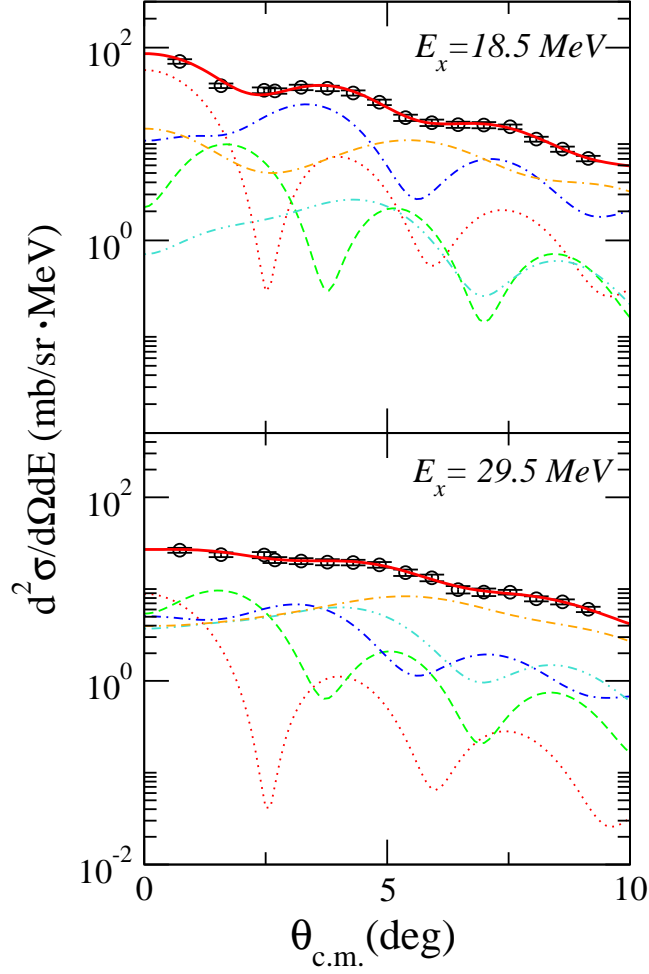


FIG. 3: Angular distributions of selected 1 MeV bins for the $^{58}\text{Ni}(\alpha, \alpha')$ reaction at 386 MeV. (a) Results for $E_x = 18.5$ MeV. The open circles are the experimental data. The lines show contributions from $L = 0$ (dotted line), $L = 1$ (dashed line), $L = 2$ (dot-dashed line), $L = 3$ (double dot-dashed line) and other higher-multipole components including IVGDR (double dash-dotted line), respectively. (b) Same as part (a), except for $E_x = 29.5$ MeV.

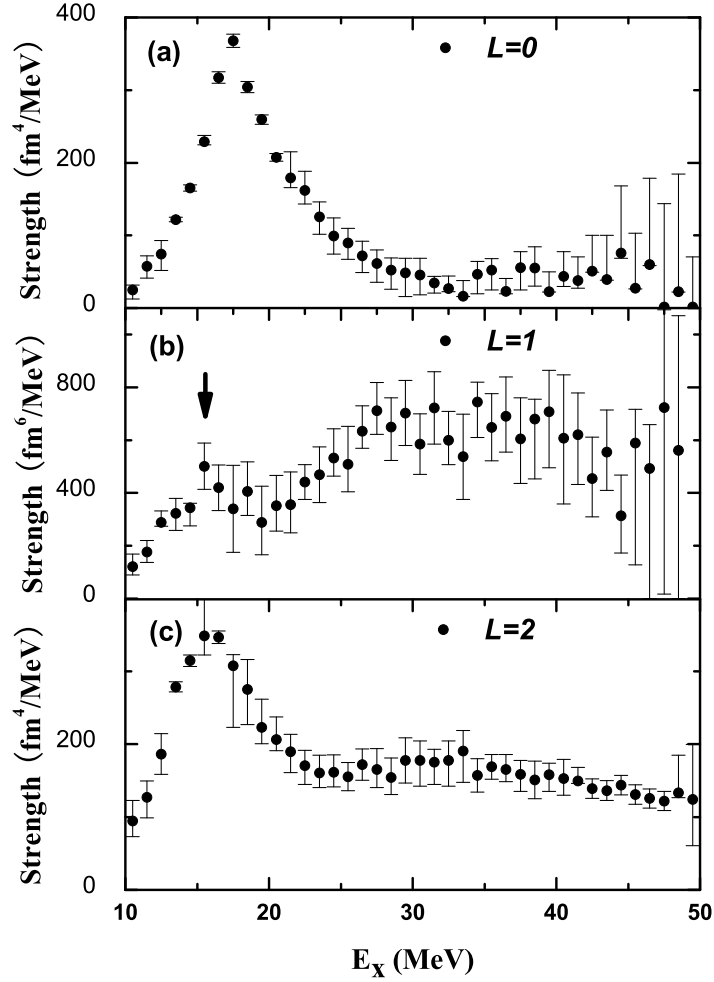


FIG. 4: Strength distributions for the $L = 0, 1,$ and 2 in ^{58}Ni . (a) ISGMR, (b) ISGDR, (c) ISGQR. The errors shown for each excitation-energy bin were estimated by changing the strength parameter for one component in order to satisfy $\Delta\chi^2$ increase by 20% while fitting with the other parameters remaining free. The low-energy component of the ISGDR is indicated by an arrow.

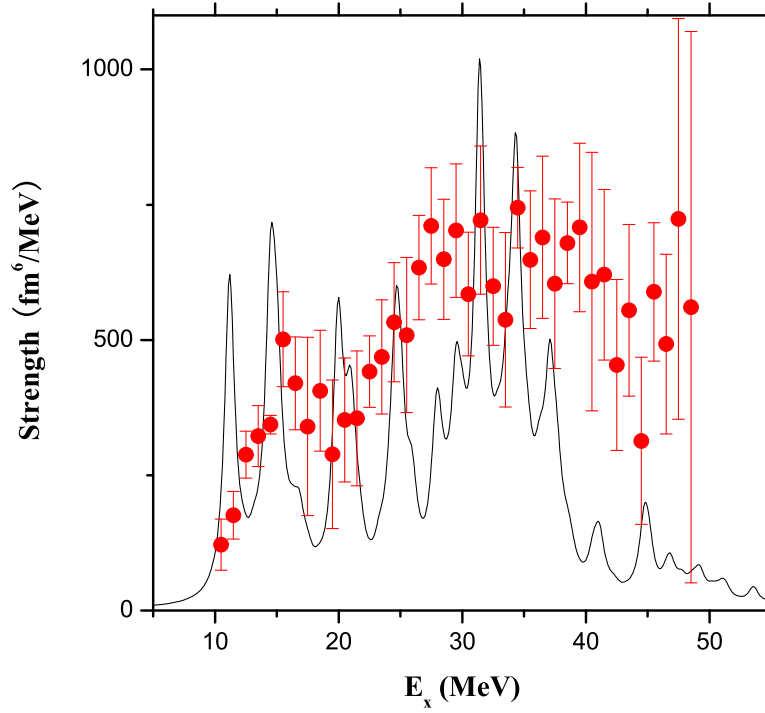


FIG. 5: Comparison of the experimental ISGDR strength distribution in ^{58}Ni with the predictions of recent QRPA calculation (continuous line) [13].